

Low-noise PPLN-based single-photon detector

Hai Xu, Lijun Ma, Oliver Slattery, and Xiao Tang*

Information Technology Laboratory

National Institute of Standards and Technology, 100 Bureau Drive, Gaithersburg MD 20899

ABSTRACT

This paper describes the detection of single photons, which have been transmitted through standard fiber at the telecom wavelength of 1310 nm. Following transmission, the 1310-nm photon is up-converted to 710 nm in a periodical-poled LiNbO₃ (PPLN) waveguide and then detected by a silicon-based avalanche photodiode (Si-APD). The overall detection efficiency of the detector is 20%. We have also characterized the sensitivity of the PPLN's efficiency to temperature and wavelength changes. We focused on the noise property of the up-conversion detector. Without classical channel co-propagation, the dark count rate is 2.2 kHz, which is lower than current up-conversion detectors by more than one order of magnitude. The up-conversion detector is then applied to a QKD system, which is characterized and is shown to have a very strong performance.

Keywords: single-photon detector, photon counting, quantum detectors, up-conversion, quantum key distribution, quantum communication, optical communication

1. INTRODUCTION

The performance of a quantum-key distribution system depends on both transmission loss and detection efficiency [1]. For current fiber systems, the transmission loss is small in the telecom wavelength window — around 0.35 dB/km at 1310 nm and 0.2 dB/km at 1550 nm. At these wavelengths, InGaAs avalanche detectors are sensitive to single photons. However, due to strong after-pulsing effects, InGaAs APDs are usually operated in gated mode, typically limiting the clock rate of the system to several MHz [2]. As a result, the sifted-key rate is also limited [3]. By comparison, silicon avalanche photo-diodes (Si-APD) have a much smaller after-pulsing effect but their detection efficiency decreases rapidly at wavelengths longer than 1000 nm [4].

To achieve both low transmission loss and good detection performance, one can apply sum frequency generation to up-convert the frequency of the received signal photons from a telecom wavelength to a short wavelength, where they can be efficiently detected by Si-APDs. By co-propagating the signal photons with a strong pump through a quasi-phase matching device such as a periodically poled LiNbO₃ (PPLN) waveguide, almost 100% of internal conversion efficiency can be achieved [5].

We developed a PPLN-based up-conversion single photon detector, the highlight of which is its low-noise feature: The dark count rate of the detector is significantly reduced when compared to previous works [5]. This low-noise feature is achieved by three key aspects of the detector: The pump wavelength is set to be longer than the signal wavelength; The pump is modulated to be a bit-synchronous pulse train; The pump noise is reduced with a proper filtering scheme. In section 2 we introduce the configuration of the PPLN-based up-conversion single-photon detector and we show the dark count rate. In section 3 we compare the dark count rates in pulse pump and continuous wave (CW) pump. In section 4 we describe the proper filtering scheme required to reduce pump noise. In section 5 we studied the wavelength and temperature sensitivity of the up-conversion efficiency. Our measurement shows the efficiency is sensitive to a wavelength change of less than 0.075 nm, *i.e.*, the detection efficiency reduces by 3 dB when the wavelength corresponding to the sum frequency of the pump and signal, λ_{sum} , deviates from the wavelength with peak efficiency, λ_{peak} , by 0.075 nm. The wavelength at peak efficiency λ_{peak} is a characteristic of the PPLN waveguide and is sensitive to

* xiao.tang@nist.gov; phone 1 301 975 2503

the waveguide temperature with a change of 0.057 nm per degree Celsius. In section 6, we apply the up-conversion detector to a B92 QKD system. We observe a secure key rate of 9.1 kbit/s over 50 km of standard single-mode fiber.

2. CONFIGURATION AND PERFORMANCE OF PPLN-BASED UP-CONVERSION SINGLE-PHOTON DETECTOR

Figure 1 shows the configuration of the up-conversion detectors that detects 1310-nm single photons. A 1557-nm CW light is modulated to form an optical pulse train, which is then amplified by an erbium-doped fiber amplifier (EDFA). An optical filter, FLT_0 , with a full-width half maximum (FWHM) of 7 nm is used to suppress noise at the output of the EDFA. The input polarization state of both the quantum input signal and the pump are adjusted by polarization controllers, PC_1 and PC_2 respectively. The amplified pump is then combined with the incoming 1306-nm quantum-channel signal by a wavelength division multiplexer (WDM) and the combined signal is sent to PPLN waveguides. The 710-nm output of PPLN is coupled to a 700-nm single mode fiber (5- μ m core), which cuts off the strong 1557-nm pump light, and is sent to Si-APDs. Before the Si-APD, we applied another filtering component FLT_1 . The FLT_1 contains two filters: a 20-nm band-pass filter and a short-pass filter. The short-pass filter attenuates the light between 730 nm and 1000 nm by more than 50 dB. This combination of filters helps to attenuate the light by more than 80 dB between 730 nm and 1000 nm, above which the filtering effect is less significant.

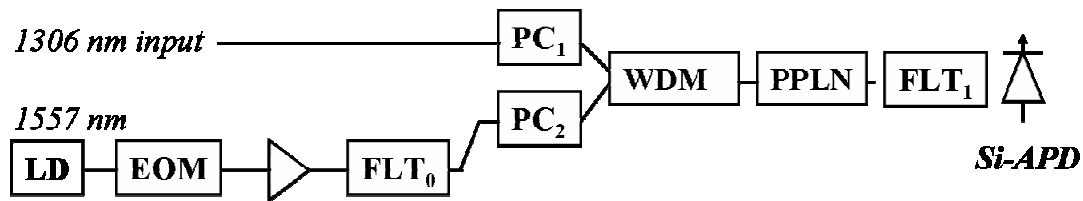


Fig. 1. Configuration of the up-conversion detectors. LD: Laser diode; EOM: Electric-optic modulator; EDFA: Erbium-doped fiber amplifier; FLT: Optical filter; PC: Polarization controller; WDM: Wavelength-division multiplexer for 1306 nm and 1556 nm; PPLN: Periodically-poled $LiNbO_3$ module.

In figure 2 we show the detection efficiency and the dark count of the detector. Both of the signal and the pump are pulse modulated. The signal is a 625-MHz random pulse train and the pump is a periodic pulse train bit-synchronized to the signal. The full width at half maximum (FWHM) of the signal and the pump pulses are 220 ps and 620 ps respectively.

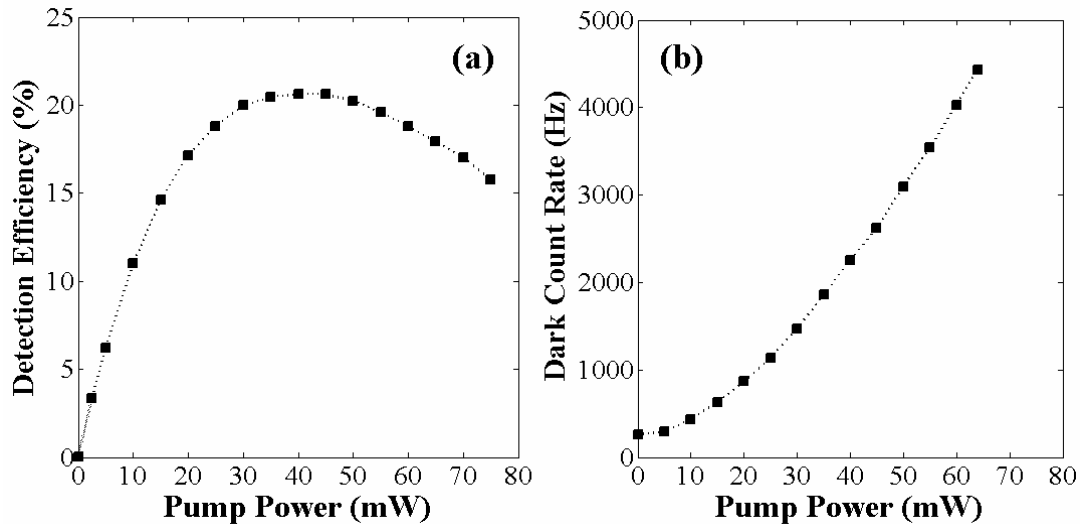


Fig. 2. The detection efficiency (a) and dark count rate (b) as a function of average pump power at the PPLN input.

The maximal detection efficiency is 20%, which corresponds to 100% of internal conversion efficiency after we exclude the component loss, waveguide coupling loss, and the 65% of detection efficiency of Si-APD. The dependency of the detection efficiency on the pump power satisfies the $\sin^2(\sqrt{\cdot})$ function [5]. The maximal efficiency is reached at the pump power of 40 mW, about 50% less than in previous works [5] due to the usage of the pulse format in the pump, as described in the next section.

The dark counts can be induced both linearly and nonlinearly. The linearly induced dark counts are the directly detected photons from the pump and classical-channel after they leak through the filter. We refer to the remaining noise photons as nonlinearly induced noise photons. The nonlinear process generating the dark counts is widely believed to be the Raman Stokes process, in which the pump generates a photon in the signal band and then up-converts this photon to the detection wavelength [6], though this has not been strictly proven. In this work, we use the signal at 1310 nm, which is shorter than the pump at 1550 nm. Because the anti-Stokes component of the Raman process is much weaker than the Stokes component, the dark count rate is significantly less than that reported previously [5, 6]. Other noise-reduction methods include the usage of the pulse modulated pump and proper filter settings as we will describe in next sections.

3. COMPARISON OF PUMP FORMATS

In a QKD system, the quantum signal is typically modulated to pulses. When the signal pulse width is significantly less than the pump pulse width, nearly all of the signal photons can be up-converted. For example, in this experiment, the rise time and the fall time are approximately 100 ps in both the signal and pump. Therefore, when we set the signal pulse width (FWHM) to 220 ps and the pump pulse width to 620 ps, the full width at 90% of the maximum of the pump pulse is larger than the full width at 10% of the maximum of the signal.

Figure 3 shows the correlation between the detection efficiency and the dark count rate in the two different pump formats — CW and pulse. In each pump format, we varied the average pump power and at each power setting we measured the conversion efficiency and dark count rate. We use the same setting as that in Sec. 2 except that in the CW case we turned off the pulse modulation. As described in Sec. 2, the 20% of detection efficiency is reached when the internal conversion efficiency of the PPLN is nearly 100%.

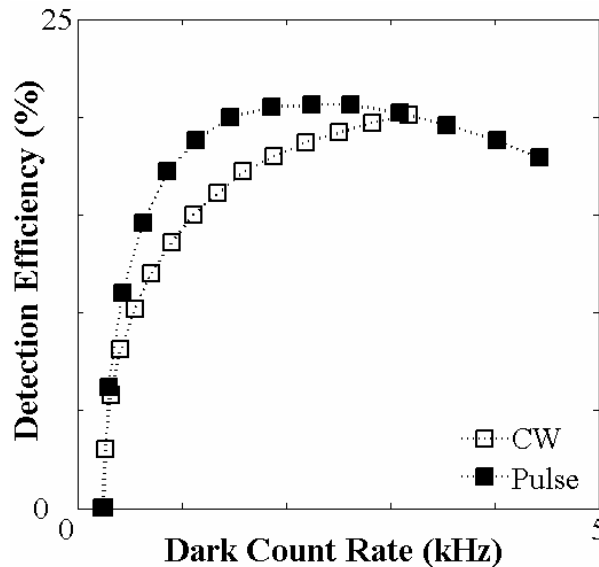


Fig. 3. The overall detection efficiency of the up-conversion single-photon detector vs. the dark count rate at the corresponding average pump power when using CW and pulse-modulated pump.

As shown in the figure, for a given detection efficiency, the dark count rate is less with the pulse pump. When the pump pulse is much wider than the signal pulse, the internal conversion efficiency of the PPLN is determined by the peak power. In this case, at a given peak pump power and thus a given detection efficiency, the dark counts increase as one increases the duty ratio (pulse width) of the pump because the dark counts now can be generated in wider time window. Consequently, at a given detection efficiency the CW light (duty ratio of 1) induces more dark counts than the pulsed pump.

Above all, the pump pulse needs to be wider than the signal pulse to achieve 100% of internal conversion efficiency. In the mean time, a wider pump pulse induces more dark counts. Therefore, there exists an optimal pump pulse width, whose value depends on the signal pulse width, timing jitter, pulse shape etc.

4. FILTERING OF THE PUMP NOISE

As shown in Fig. 2, we attain dark count rates around several thousands counts per second, which is significantly lower than those of shorter-wavelength-pump schemes [5, 6]. In achieving such a low dark count rate, the ‘post-filtering’ after PPLN (FLT₁) alone is not sufficient and the optical band-pass filter before PPLN (FLT₀) is also important. FLT₀ blocks a large amount of EDFA noise, particularly the noise between 1000 nm and 1300 nm as shown in Fig. 4a. The noise in this region can induce a large amount of noise photons which cannot be blocked by FLT₁, see Fig. 4b. The WDMs located before the PPLNs are specified by the manufacturer to filter out the light between 1300 nm and 1330 nm by more than 20 dB but they do not block the noise between 1000 nm and 1300 nm.

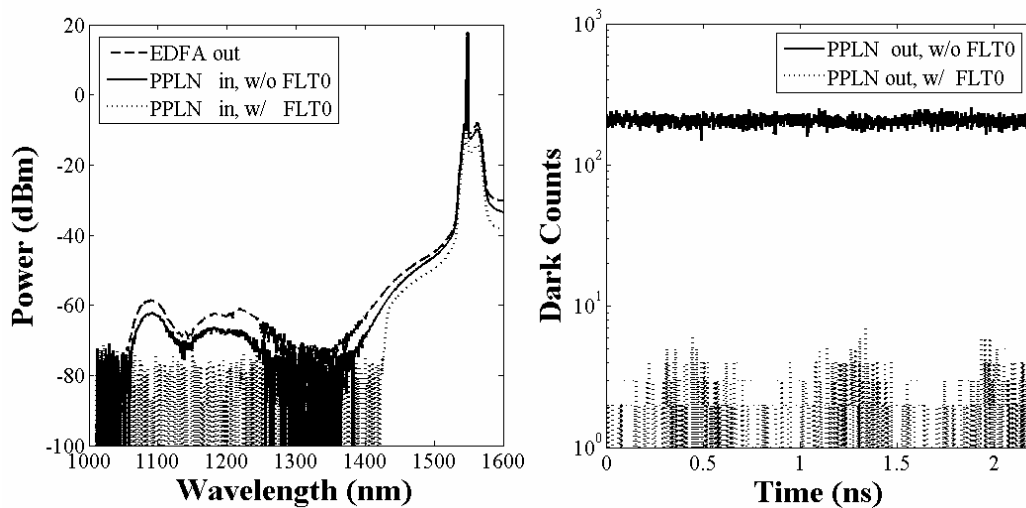


Fig. 4. (a) The optical spectrum of the pump light immediately after the EDFA and at the input of the PPLN, each measured with and without FLT₀. (b) The photon counts over time collected by a photon counting card at the output of two up-conversion detectors, each with and without FLT₀. During the measurement, no signal at 1306 nm was present and only the pump light was sent to the PPLN. The pump power was approximately 40 mW before each PPLN.

As shown in Fig. 4b, the dark count rate is 1.1×10^6 counts/s without FLT₀ and 2200 counts/s with FLT₀. An EDFA noise photon can be directly detected by the Si-APD (linear process) or it can be up-converted by the 1550-nm pump to a photon around 710 nm and then detected by the Si-APD (nonlinear process). The nonlinearly induced dark count also include the up-converted 1310-nm noise photon induced by the Raman process inside the PPLN. The linearly induced dark counts resemble white noise while the nonlinearly induced dark counts exhibit the pulse pattern of the pump. As shown in the figure, without FLT₀ most of the PPLN’s dark counts are induced linearly from the EDFA noise because the filter FLT₁ and the 700-nm single-mode fiber cannot block the light between 1000 nm and 1300 nm. Therefore, a large amount of noise photons reach the Si-APD inducing a large amount of white-noise-like dark counts. Using FLT₀ to suppress the EDFA noise, we greatly reduced these dark counts, as shown in Fig. 4b. In this case, most of the dark counts are nonlinearly induced showing the pulse pattern.

Overall, using pulsed pump light at 1557 nm and a signal at 1306 nm, and applying proper filtering, we achieved substantially lower dark count rates in the up-conversion detector. When the pump power is set to 40 mW, the dark count rate is 2.2×10^3 counts/s. Such dark count rates are nearly two orders of magnitude lower than that given by the 1310-nm pump scheme [5].

5. WAVELENGTH AND TEMPERATURE SENSITIVITY OF PPLN

The quasi-phase matching condition in the PPLN is satisfied at a particular up-conversion wavelength λ_{peak} , at which peak up-conversion efficiency is achieved. When the wavelength corresponding to the sum-frequency of the pump and the signal, λ_{sum} , deviates from λ_{peak} the up-conversion efficiency is reduced. The up-conversion wavelength λ_{peak} is also temperature sensitive. Therefore, one or both of the pump and the signal wavelength, as well as the PPLN temperature needs to be accurately tuned to achieve the maximal up-conversion efficiency. Moreover, the up-conversion efficiency could be reduced when the linewidth of the pump or signal becomes wider than the spectral width of the up-conversion process.

To investigate the spectral and the temperature sensitivity of the up-conversion, we sent a 1 mW CW 1306-nm light with a linewidth less than 10 MHz into the PPLN. Moreover, we turn off the 1557-nm laser diode so that the amplified spontaneous emission (ASE) noise from the EDFA acts as the pump. We measured the spectrum at the output of PPLN at different temperatures from 50 °C to 70 °C using optical spectrum analyzer (OSA) with a resolution bandwidth of 0.05 nm. The output spectrum is normalized to the peak power after we subtracted the ASE spectrum. The result is shown in Fig. 5.

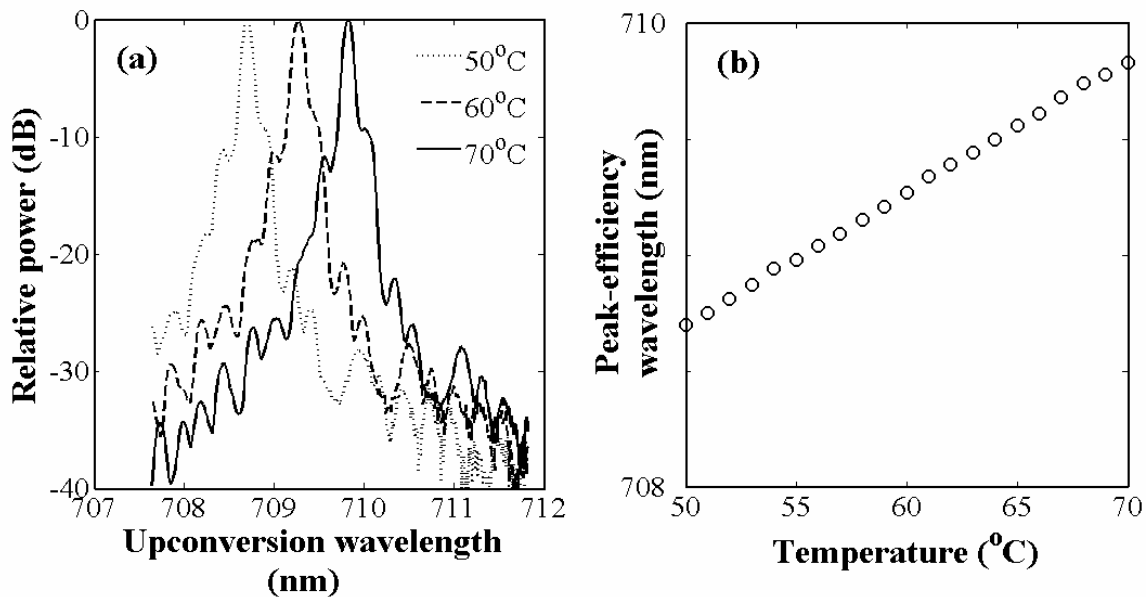


Fig. 5 (a) The normalized output spectrum of the PPLN at the different temperatures shown in inset. (b) The up-conversion wavelength λ_{peak} as a function of temperature.

As shown in Fig. 5(a), the spectral width of the up-conversion is 0.15 nm. As a result, when λ_{sum} deviates from λ_{peak} by 0.075 nm, the up-conversion efficiency is reduced by half or 3dB. Note that the actual spectral width may be even less considering 0.05 nm resolution of OSA. Consequently, the wavelength of the sum frequency λ_{sum} cannot be different from λ_{peak} by more than 0.075 nm, *i.e.*, $|\lambda_{\text{sum}} - \lambda_{\text{peak}}| < 0.075$ nm, in order to achieve high up-conversion efficiency. Such quasi-phase matching condition can be achieved by adjustment of the pump/signal wavelength (adjustment of λ_{sum}) or the temperature of the PPLN waveguide (and consequently the peak wavelength λ_{peak}), as shown in Fig. 5(b). With a 20 degree temperature variation, the peak –efficiency wavelength λ_{peak} linearly varies by approximately 1.1 nm.

6. APPLICATION TO QKD SYSTEM

We applied the up-conversion detector to a QKD system. The quantum key is encoded by 1310-nm photons with the B92 protocol, as shown in the Fig. 6. The QKD system uses a custom printed circuit board with a field-programmable gate array (FPGA) to generate a random stream of quantum key data and to transmit and receive the classical data, which will be encoded and decoded by the quantum key. The classical data is carried by the optical signal in the 1550-nm band.

To polarization-encode the quantum channel from the random quantum key, we first modulate a 1306-nm CW light into a 625-MHz pulse train which is evenly split into two polarization channels. Each pulse train is further modulated by one of two complementary 625-Mbit/s quantum channel data streams. The two quantum channels are combined by a 45-degree polarization-maintaining combiner and attenuated to a mean photon number of 0.1 per bit, then multiplexed with the classical channel and sent to a standard single-mode fiber.

At Bob, another WDM is used to demultiplex the quantum and the classical channels. The quantum channel is polarization-decoded and detected by the up-conversion single-photon detectors, generating the raw key. Bob's board informs Alice of the location of the raw keys via the classical channel. After reconciliation and error correction, Alice and Bob obtain a common version of the secure keys, which are further used to encode and decode the classical signal.

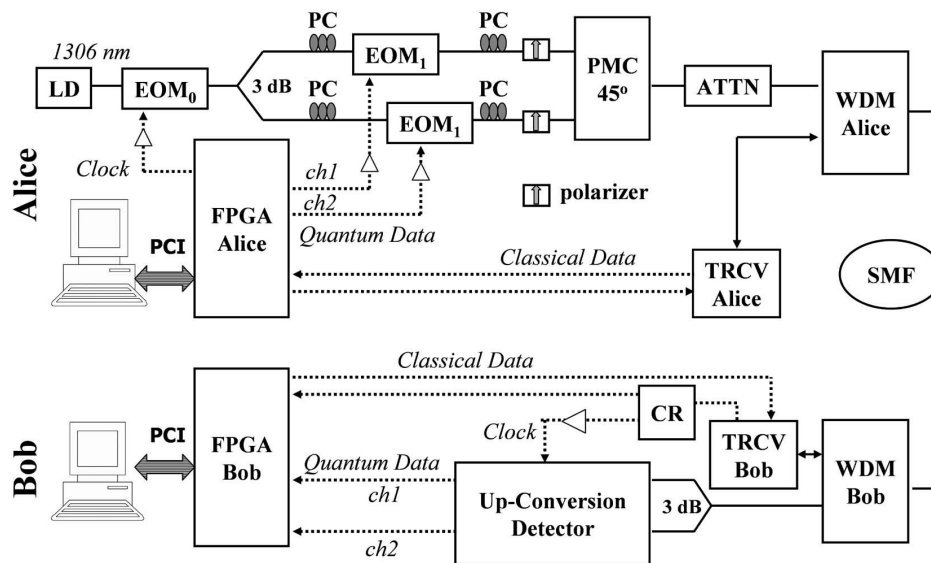


Fig. 6. The B92 polarization coding QKD system. LD: Laser diode; EOM: Electric-optic modulator; PC: Polarization controller; PMC-45°: Polarization maintaining combiner that combines two light signals that are separated by 45 degrees; ATTN: Optical attenuator; WDM: Wavelength-division multiplexer; SMF: Standard single-mode fiber; TRCV: Optical transceiver; CR: Clock recovery module; FPGA: Custom printed circuit board controlled by a field-programmable gate array; PCI: PCI connection; Up-conversion detector: See Fig. 2; Dotted line: Electric cable; Solid line: Optical fiber.

The system performance is shown in Fig. 7. During the measurements, the pump power is fixed at 40 mW. The sifted-key rate is 2.5 Mbit/s with a back-to-back connection (0 km), 1 Mbit/s at 10 km, and 60 kbit/s at 50 km. The error rate is approximately 3% for back-to-back, remains below 4% for up to 20 km, and reaches 8% at 50 km. The finite extinction ratio of the modulator and the timing jitter of the system induce a background error rate of approximately 2.5% and the remaining portion of the error rate is from the dark counts. In Fig. 7(b) we use our experimentally measured sifted-key rate (SKR) and error rate (ER) to calculate the secure key rate using two different algorithms, [7, 8] and [9]. Both algorithms yielded similar results. We were able to generate secure keys in real time and used them as a one-time-pad for a continuous 200-kbit/s encrypted video transmission over 10 km, although we incurred periodic stalling due to the limited buffer size.

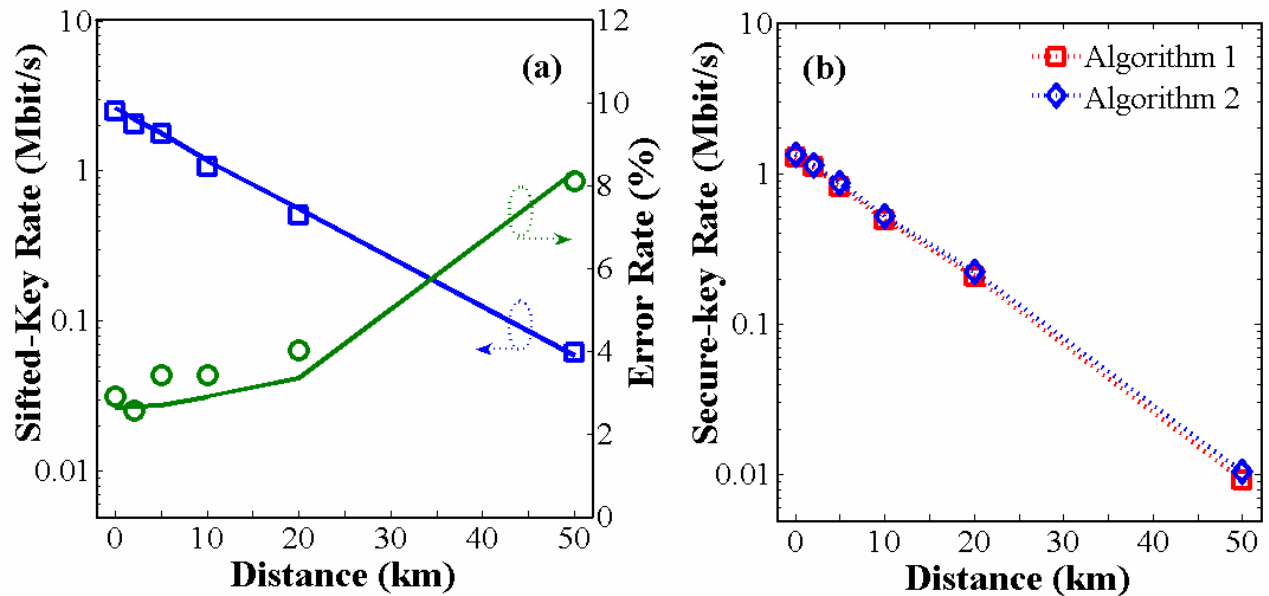


Fig. 7. The system performance of the B92 polarization-coding QKD system with the 1557-nm up-conversion detector. (a) Left blue line: the sifted-key rate calculated; Left blue square: the sifted-key rate measured in the experiment; Right green line: the error rate calculated. Right green circle: the error rate measured in the experiment. (b) The secure-key rate calculated using algorithm 1 [7, 8] and algorithm 2 [9]. The calculation is coded on the sifted-key rate and error rate measured in the experiment.

Although we fixed the pump power close to the maximum up-conversion efficiency, the error rate remains small until 20 km due to the low dark count rate of the up-conversion detector. A secure-key rate of approximately 9.1 kbit/s is achievable at 50 km.

7. CONCLUSION

We developed a low-noise PPLN-based up-conversion detector. The low-noise feature is achieved with the pump at a wavelength longer than the quantum signal, a pulse modulation format, and a proper noise filtering setting. We also investigated the wavelength and the temperature sensitivity of the up-conversion in the PPLN waveguide. We have applied the up-conversion detector to a B92 polarization-coding QKD system and observed approximately 500 kbit/s and 9.1 kbit/s of secure-key rates at 10 km and 50 km, respectively. The system can generate secure keys in real time for one-time-pad encryption of continuous 200 kbit/s encrypted video transmission over 10 km. More importantly, with the low dark count rate in this up-conversion detector we expect significant improvements in the system performance when more advanced protocols, better PPLN modules, and higher data rates are applied.

ACKNOWLEDGMENT

The authors acknowledge the support of the DARPA QuIST program and NIST Quantum information Initiative program.

REFERENCES

1. N. Gisin, G. Ribordy, W. Tittel, and H. Zbinden, "Quantum cryptography," *Rev. Mod. Phys.* **74**, pp. 145–195, (2002).
2. <http://www.idquantique.com>
3. C. Gobby, Z. L. Yuan, and A. J. Shields, "Unconditionally secure key distribution over 50 km of standard telecom fiber," *Electron. Lett.* **40**, pp. 1603- 1605, (2004)
4. <http://optoelectronics.perkinelmer.com/catalog/Product.aspx?ProductID=SPCM-AQR-14>.
5. C. Langrock, E. Diamanti, R. V. Roussev, Y. Yamamoto, M. M. Fejer, and H. Takesue, "Highly efficient single-photon detection at communication wavelengths by use of upconversion in reverse-proton-exchanged periodically poled LiNbO₃ waveguides," *Opt. Lett.* **30**, pp. 1725-1727, (2005).
6. R. T. Thew, S. Tanzilli, L. Krainer, S. C. Zeller, A. Rochas, I. Rech, S. Cova, H Zbinden and N. Gisin, "Low jitter up-conversion detectors for telecom wavelength GHz QKD," *New J. Phys.* **8**, 32, pp. 1–12 (2006).
7. A. Mink, X. Tang, L. Ma, T. Nakassis, B. Hershman, J. C. Bienfang, D. Su, R. Boisvert, C. W. Clark and C. J. Williams, "High speed quantum key distribution system supports one-time pad encryption of real-time video," at Proc. of SPIE 6244-22, Orlando, FL, Apr., 2006.
8. A. Nakassis, J. Bienfang, and C. Williams, "Expeditious reconciliation for practical quantum key distribution," in Defense and Security Symposium: Quantum Information and Computation II, Proc. SPIE 5436, pp. 28-35, (2004).
9. N. Lütkenhaus, "Security against individual attacks for realistic quantum key distribution," *Phys. Rev. A* **61**, 052304, pp.1–10, (2000).